Journal of Instrumentation

Experimental ion mobility measurements in Ar-N_2

Published by IOP Publishing for Sissa Medialab

Received: *July 20, 2018*
Accepted: *October 12, 2018*
Published: *November 20, 2018*

Experimental ion mobility measurements in Ar-N_2

M.A.G. Santos,[a,b] **A.F.V. Cortez,**[a,b,1] **J.M.C. Perdigoto,**[a] **J. Escada,**[a,b] **R. Veenhof,**[c,d,f] **P.N.B. Neves,**[e] **F.P. Santos,**[a,b] **C.A.N. Conde**[a,b] **and F.I.G.M. Borges**[a,b]

[a] *Department of Physics, Faculty of Science and Technology, University of Coimbra, Rua Larga, Coimbra, 3004-516 Portugal*
[b] *Laboratory of Instrumentation and Experimental Particle Physics — LIP, Rua Larga, Coimbra, 3004-516 Portugal*
[c] *CERN PH Department, Geneve 23, CH-1211 Switzerland*
[d] *Department of Physics, Uludag University, Bursa, 16059 Turkey*
[e] *Closer Consultoria, LDA, Lisboa Codex, Portugal*
[f] *National Research Nuclear University MEPhI, Kashirskoe Highway 31, Moscow, Russia*

E-mail: andre.f.cortez@gmail.com

Abstract: Data on ion mobility is important to improve the performance of large volume gaseous detectors, since the detector signal can be influenced by the drift of the ions, namely in the cases where charge multiplication is used, for example in Multi-Wire Proportional Chambers (MWPCs) and in some Time Projection Chambers (TPCs). In the present work the results for the ion mobility measurements in Ar-N_2 mixtures are presented, using an experimental setup and method already tested in previous work. The results for this mixture show the presence of only one peak for all gas ratios of Ar-N_2, for reduced electric fields, E/N, in the range of 10–25 Td (2.4–6.1 kV·cm^{-1}·bar^{-1}), and 8 Torr (10.6 mbar) pressure, at room temperature.

Keywords: Charge transport and multiplication in gas; Gaseous detectors; Ion sources (positive ions, negative ions, electron cyclotron resonance (ECR), electron beam (EBIS)); Ionization and excitation processes

[1] Corresponding author.

https://doi.org/10.1088/1748-0221/13/11/P11016

2018 JINST 13 P11016

Contents

2018 JINST 13 P11016

1 Introduction

Measuring the mobility of ions in gases is relevant in several areas from physics to chemistry, e.g. in gaseous radiation detectors modelling and in understanding the pulse shape [1–4], since their mobility can affect the performance of these detectors [3] as they influence the rate capability and signal formation of detectors, e.g., of the Multi-Wire Proportional Chambers (MWPCs) [5]. The choice of the gas mixture for most of these detectors is determined by several characteristics such as high electron/ion velocity and low electron diffusion.

The experimental setup used in the present work (described in detail in [6]) allows the measurement of ion mobility in gas mixtures. Initially thought for high pressure, it was converted into a low pressure gas system. Lowering the operation pressure provided a wider scope of application and more detailed information on the fundamental processes involved in the ion transport and also allowed to reduce the inherent operation cost. Still, the results have been consistently in accordance with data obtained at higher pressures [7].

In this work, the mobility of ions in Ar-N_2 gas mixtures was measured at a pressure of 8 Torr (10.6 mbar) and for reduced electric fields commonly used in gaseous detectors, 15 Td (3.6 $kV{\cdot}cm^{-1}{\cdot}bar^{-1}$), extending previous studies developed in our group for other gases [6–22].

1.1 Ion mobility

Under a weak and uniform electric field a group of ions will eventually reach a steady state. In this conditions, the average velocity of this group of ions, also known as drift velocity v_d, is proportional to the electric field intensity [4]:

$$v_d = KE \tag{1.1}$$

where K is the mobility of the ions, expressed in units of $cm^2{\cdot}V^{-1}{\cdot}s^{-1}$ and E the intensity of the drift electric field. The ion mobility, K, is normally expressed in terms of the reduced mobility K_0,

$$K_0 = KN/N_0 \tag{1.2}$$

with N the gas number density and N_0 the Loschmidt number ($N_0 = 2.68678 \times 10^{19}\,\mathrm{cm}^{-3}$ for 273.15 K and 101.325 kPa according to NIST [23]). The mobility values are commonly presented as a function of the reduced electric field E/N in units of Townsend (1 Td=$10^{-17}\,\mathrm{V{\cdot}cm}^2$).

1.2 Langevin's theory

According to Langevin's theory [24], one limiting value of the mobility is reached when the electrostatic hard-core repulsion becomes negligible compared to the neutral polarization effect [25]. This limit is given by the following equation,

$$K_{\mathrm{pol}} = 13.88 \left(\frac{1}{\alpha\mu}\right)^{\frac{1}{2}} \tag{1.3}$$

where α is the neutral polarisability in cubic angstroms ($\alpha = 1.64\,\text{Å}^3$ for Ar [26] and $\alpha = 1.95\,\text{Å}^3$ for N_2 [27]) and μ is the ion-neutral reduced mass in unified atomic mass units. Although the Langevin limit only applies rigorously for real ion-neutral systems in the double limit of low E/N and low temperature, it still predicts the low-field mobility at room temperature with relatively good accuracy [25], which is the case of our experimental conditions. Although generally accepted, Langevin theory has some known limitations in its application, since it fails to provide correct values for the ion's mobility in some cases, namely for gases with low polarizability or for very large molecules [7].

1.3 Blanc's law

In binary gaseous mixtures, Blanc's law has proven to be most useful when determining the ions' mobility. According to this law, the reduced mobility of the ion in the binary mixture, K_{mix}, can be expressed as follows:

$$\frac{1}{K_{\mathrm{mix}}} = \frac{f_1}{K_{\mathrm{g1}}} + \frac{f_2}{K_{\mathrm{g2}}} \tag{1.4}$$

where K_{g1} and K_{g2} are the reduced mobility of that same ion in an atmosphere of 100% of gas #1 and #2, respectively and f_1 and f_2 are the molar fraction of each gas in the binary mixture [28].

2 Method and experimental setup

The mobility measurements were obtained using the experimental system described in [6]. A UV flash lamp with a frequency of 10 Hz emits photons that impinge on a 250 nm thick CsI film deposited on the top of a GEM that is inside a gas vessel. The photoelectrons released from the CsI film are guided through the GEM holes, ionizing the gas atoms/molecules along their paths. While electrons are collected at the GEM bottom electrode, cations formed will drift across a uniform electric field region towards a double grid; the first of these acts as a Frisch grid while the second, at ground voltage, collects the ions' charge. A pre-amplifier is used to convert the charge collected into a voltage signal, and the time spectra are recorded in a digital oscilloscope. After electronic background subtraction from the signal, gaussian curves are fitted to the time-of-arrival spectra from which the peak centroids are obtained. Since the peaks' centroid correspond to the average drift time of the ions along a known fixed distance (4.273 cm), the drift velocity and mobility can then be

2018 JINST 13 P11016

calculated. One important feature of the system is the capability of controlling the voltage across the GEM (V_{GEM}), which limits the maximum energy gained by the electrons as they move across the GEM holes, narrowing the variety of primary ions possibly produced. Identifying the primary ions will allow to pinpoint secondary reaction paths that lead to the identification of the detected ions. This experimental setup has already provided correct and consistent results for several gases and their mixtures.

Since impurities play an important role in the ions' mobility, before each experiment the vessel was vacuum pumped down to pressures of 10^{-6} to 10^{-7} Torr and a strict gas filling procedure was carried out. No measurement was considered until the signal stabilised, and all measurements were done in a 2–3 minutes time interval to ensure minimal contamination of the gas mixture, mainly due to outgassing processes.

The method described together with the knowledge of the ions' dissociation channels, the product distribution and rate constants of the possible secondary reactions represent a valid solution to the ion identification problem.

3 Results and discussion

The mobility of the ions originated in Ar-N_2 mixtures has been measured at different reduced electric fields E/N (10 Td and 25 Td) and 8 Torr pressure at room temperature (293 K).

3.1 Argon-nitrogen (Ar-N_2) mixtures

In argon-nitrogen (Ar-N_2) mixtures, only one peak is observed in the different time spectra throughout the entire mixture range studied, with a bump appearing on the left side of the peak for Ar concentrations above 70%, as seen in figure 1. The drift spectra for several Ar-N_2 mixtures (5%, 50%, 70% and 95% of Xe) are shown in figure 1, at a pressure of 8 Torr, temperature of 293 K, reduced electric field of 15 Td and V_{GEM} of 25 V. There are three striking changes that result from the increase in Ar concentration: the first is a decrease observed in the mobility of ions, the second is an increase in the peak amplitude and the third is the appearance of the referred bump, for Ar concentrations above 70%.

To understand which ions are responsible for the peak and bump observed, a Monte Carlo simulation was performed, to have an insight on how the proportion of the primary ions formed (from N_2 and Ar ions) evolve with the mixture composition. This information together with the reaction rates available in literature, allows to obtain a clear picture of the ions drifting in this mixture.

The Monte Carlo simulation code used is described in detail in [31], and as in [21], a uniform field was considered inside the GEM holes, between anode and cathode. Although this is an approximation of the real field geometry, it has already provided valuable information for this purpose in previous studies. The simulation reproduces the drift of 10^8 photoelectrons released from a CsI photocathode into Ar-N_2 mixtures and their collisions with the gas atoms/molecules (at the typical pressure of 8 Torr and temperature of 293 K) until they reach the anode, 50 μm away, and calculates the proportion of primary ions (N_2^+ and Ar^+) produced by these electrons for the different gas mixtures.

2018 JINST 13 P11016

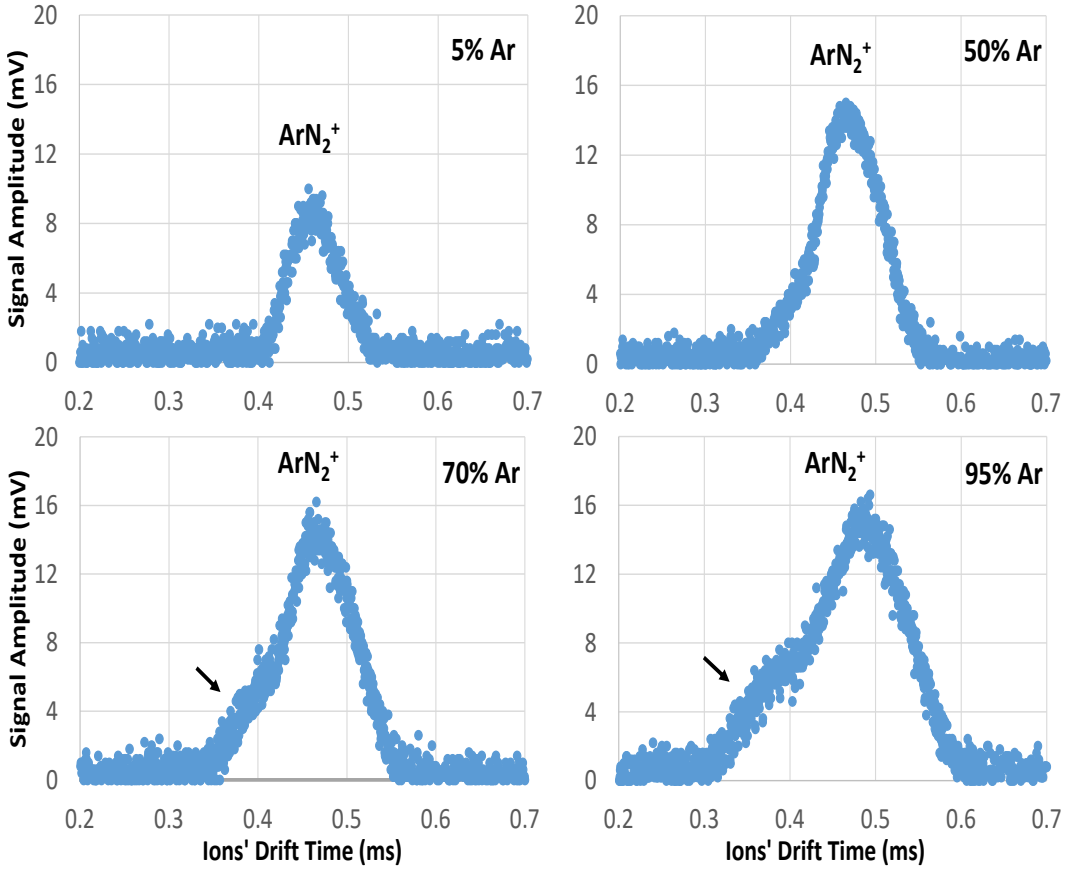

Figure 1. Time-of-arrival spectra averaged over 128 pulses for several Ar-N_2 mixtures (5%, 50%, 70% and 95% of Ar) at a pressure of 8 Torr, temperature of 293 K and for a reduced electric field of 15 Td with a voltage across GEM of 25 V (background noise subtracted). The arrow indicates the position of the appearing bump.

The cross-sections used in the simulation code are displayed in figure 2. For the scattering of electrons by Ar atoms these are the same as those adopted in [32]. For N_2 molecules, cross-sections used are based on the data from [33, 34]. For rotational excitation, data was taken from [33, 35]; superelastic collisions corresponding to these rotational transitions were taken into account, considering the principle of detailed balance. Regarding vibrational excitation, data from [36] was used to complement data from [33]. Electron dissociative attachment cross-section was taken from [37]. For electronic excitation, the partial cross-sections were taken from [34]. For ionization, the simulation used the partial cross-sections for N_2^+ and N^+ production from [33]. All electron collisions with molecules are assumed to be isotropic, however anisotropy of elastic scattering is accounted for using momentum transfer cross-section [33] instead of integral.

The simulation results obtained are displayed in figure 3. According to these results, N_2^+ ions are produced more abundantly up to about 35% Ar, while above this concentration Ar^+ ions are the ones preferentially produced. Knowing the ions' relative initial abundance and comparing the different reaction rates summarized in table 1, it can be concluded that the reactions leading to the formation of ArN_2^+ are faster than any other competing channel, which means that in our experimental conditions the formation of ArN_2^+ is favoured.

2018 JINST 13 P11016

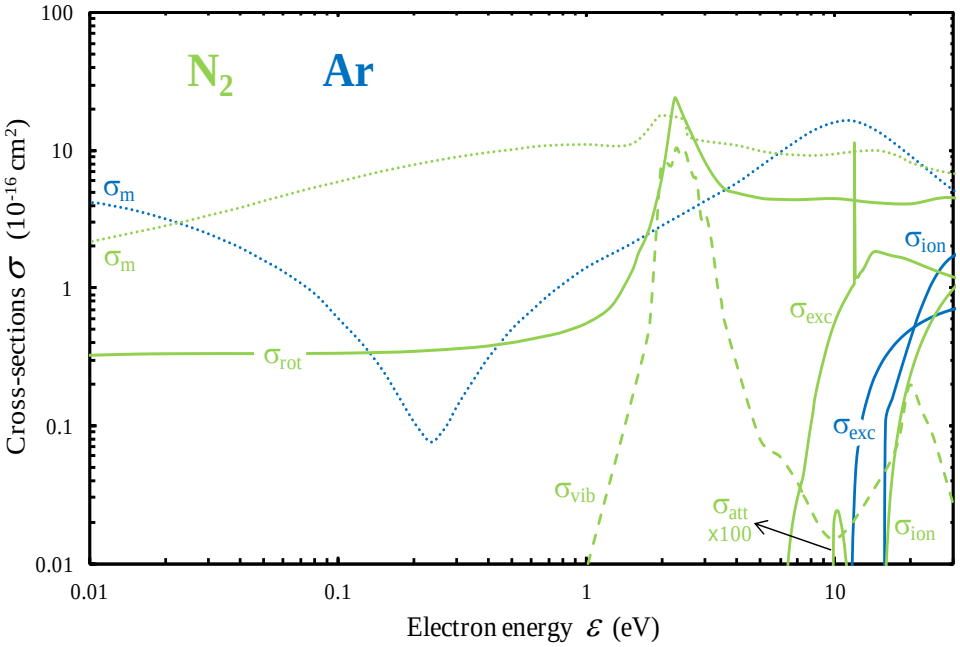

Figure 2. Electron scattering cross-sections in Ar (blue) and N_2 (green): elastic momentum transfer (σ_m); rotational excitation (σ_{rot}); vibrational excitation (σ_{vib}), electron attachment (σ_{att} multiplied by 100); electronic excitation (σ_{exc}); ionization (σ_{ion}).

Table 1. Summary of possible reactions and respective rate constants (references on the last column).

Reaction	Rate Constant	Ref.
$Ar^+ + Ar \rightarrow Ar + Ar^+$	4.6×10^{-10} cm^3·s^{-1}	[7]
$Ar^+ + 2Ar \rightarrow Ar_2^+ + Ar$;	2.2×10^{-31} cm^6·s^{-1}	[38]
$Ar^+ + N_2 \rightarrow N_2^+ + Ar$	1.1×10^{-11} cm^3·s^{-1}	[39–41]
$Ar_2^+ + N_2 \rightarrow ArN_2^+ + Ar$	2.0×10^{-11} cm^3·s^{-1}	[42]
$N_2^+ + N_2 + M \rightarrow N_4^+ + M$ (M either Ar or N_2)	5.5×10^{-29} cm^6·s^{-1}	[43]
$N_2^+ + Ar \rightarrow Ar^+ + N_2$	2.0×10^{-13} cm^3·s^{-1}	[39, 40]
$N_4^+ + Ar \rightarrow ArN_2^+ + N_2$	1.4×10^{-12} cm^3·s^{-1}	[42]
$ArN_2^+ + Ar \rightarrow Ar_2^+ + N_2$	1.0×10^{-12} cm^3·s^{-1}	[42]
$ArN_2^+ + N_2 \rightarrow N_4^+ + Ar$	3.0×10^{-13} cm^3·s^{-1}	[42]

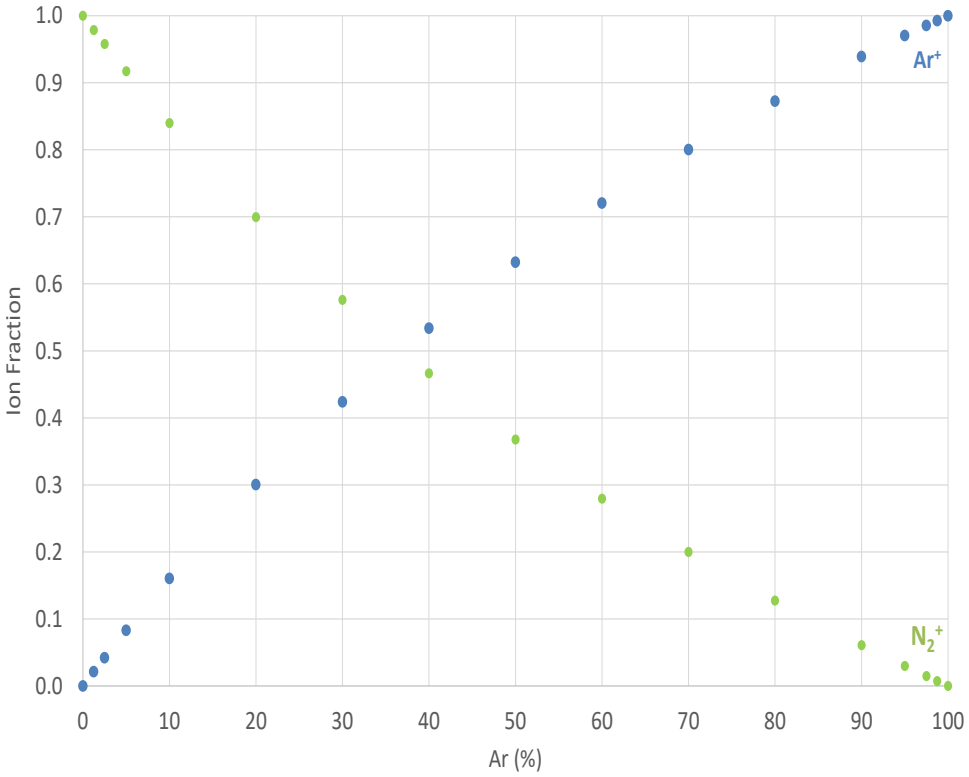

Figure 3. Results from Monte Carlo simulation for the relative production of primary ions in the GEM as a function of the relative abundance of Ar-Ar^+ (blue) and N_2^+ (green).

However, in the very low and very high Ar concentration limit, a transition is expected to occur in the dominant ion. For very low Ar concentrations, where the production of N_2^+ (primary ion) is predominant, the dominant ion, N_4^+, is expected to change gradually to ArN_2^+, when increasing Ar concentration, while for very high Ar concentrations, ArN_2^+ gradually gives way to Ar_2^+, when increasing Ar concentration. The appearance of a bump at the left side of the main peak for Ar concentrations above 70% might be due to a hetero-nuclear associative ionization of the molecule involving a highly excited state of the Ar atom and a N_2 molecule [42], expressed by:

$$Ar^* + N_2 \rightarrow ArN_2^+. \tag{3.1}$$

This reaction leads to the formation of the same ion product, ArN_2^+, but through a different channel. This being the case, this ion should in fact appear at the left side of the main peak, as ArN_2^+ will be always the same drifting ion, while through the other channel (involving Ar_2^+), its mobility (ArN_2^+) will be affected by the predecessor ions (Ar^+ and Ar_2^+) which have a lower mobility. This seems a plausible explanation for the bump, since from the Monte Carlo simulation we concluded that about 10% of the total Ar^* produced in the GEM holes have enough energy to originate ArN_2^+ ions.

In figure 4 the reduced mobility obtained for the ions produced in Ar-N_2 mixtures is plotted as a function of Ar percentage, for 8 Torr and 15 Td, at room temperature (293 K), together with Blanc's law prediction for N_4^+ (red dashed line), Ar_2^+ (orange dashed line) and ArN_2^+ (green dashed line). K_{g1} and K_{g2} in Blanc's law (eq. (1.4)), were obtained either using experimental values from literature or, when not possible, from Langevin formula (eq. (1.3)). Figure 4 shows that the ion

2018 JINST 13 P11016

mobility experimentally obtained generally follows, within error bars, Blanc's law prediction for the most abundant ion, ArN_2^+, for most of the Ar percentages studied. In fact, from pure N_2 up to 5% Ar, the ion observed displays a considerable decrease in mobility which reflects the change from N_4^+ to ArN_2^+ in the final ion. For Ar concentration above 10%, the mobility is consistent with Blanc's law prediction for ArN_2^+, deviating towards Ar_2^+ for Ar concentrations above 80%.

The slight differences observed in the drift time from pure N_2 up to 5% Ar and from pure Ar down to 80% are related with the slower production of ArN_2^+ at these concentrations conditions, that, throughout its drift, has its mobility affected by the predecessor ions, N_2^+ and Ar^+, resulting in an increase (N_2^+) or decrease (Ar^+) in the mobility of ArN_2^+. Due to the great uncertainties associated with a Gaussian fitting of the bump, this was not considered in the analysis.

Table 2 summarizes the results. No significant variation of the mobility was observed for the E/N range studied (10–25 Td).

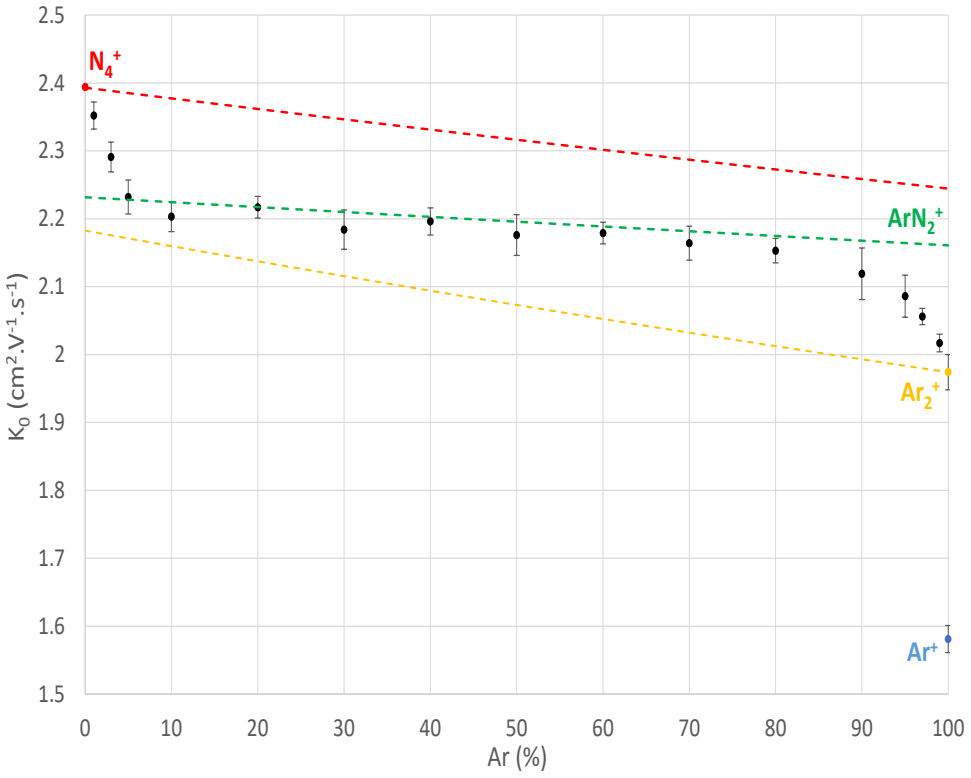

Figure 4. Reduced mobility of the ions produced in the Ar-N_2 mixture for a pressure of 8 Torr and for a E/N of 15 Td at room temperature. The dotted lines represent the mobility values expected from Blanc's law for N_4^+ (red), Ar_2^+ (orange) and ArN_2^+ (green).

2018 JINST 13 P11016

Table 2. Mobility of the ions observed for the Ar-N_2 mixture ratios studied, obtained for E/N of 15 Td, at 8 Torr and 293 K.

Ar-N_2 Mixture % of Ar	Mobility ($cm^2 \cdot V^{-1} \cdot s^{-1}$)
1%	2.35 ± 0.02
3%	2.29 ± 0.02
5%	2.23 ± 0.03
10%	2.20 ± 0.01
20%	2.22 ± 0.02
30%	2.18 ± 0.03
40%	2.19 ± 0.02
50%	2.18 ± 0.03
60%	2.18 ± 0.02
70%	2.16 ± 0.03
80%	2.15 ± 0.02
90%	2.12 ± 0.04
95%	2.09 ± 0.03
97%	2.06 ± 0.01
99%	2.02 ± 0.01

4 Conclusion

In the present work we measured the reduced mobility of ions originated by electron impact in Ar-N_2 mixtures at pressures ranging from 6 to 8 Torr, low reduced electric fields (10–25 Td) and different mixture ratios.

The experimental results show that, from pure N_2 to pure Ar and concentrations in between, only one peak is observed in all drift spectra. The ion responsible is ArN_2^+, as confirmed by Blanc's law, except for concentrations below 5% Ar and above 80% Ar, where a gradual change from the expected theoretical mobility of ArN_2^+ to N_4^+ and Ar_2^+ was observed, as would be expected. For concentrations above 70% of Ar, a bump emerged on the left side of the peak, which was attributed also to ArN_2^+, yet produced through hetero-nuclear associative ionization, involving highly excited Ar states and the neutral N_2. This hypothesis was consistent with the higher mobility of this bump, and corroborated by the Monte Carlo simulation.

The mobilities calculated did not display a significant dependence with E/N for the values used in this work (10–25 Td).

Future work is expected with different gaseous mixtures of known interest such as: Ar-iC_4H_{10}, Ar-CF_4-iC_4H_{10} and Ne-CF_4.

2018 JINST 13 P11016

Acknowledgments

This work was supported by the RD51 Collaboration/CERN, through the common project "Measurement and calculation of ion mobility of some gas mixtures of interest". A.F.V. Cortez received a Ph.D. scholarship from FCT-Fundação para a Ciência e Tecnologia (SFRH/BD/52333/2013). José Escada was supported by FCT-Fundação para a Ciência e Tecnologia (SFRH/BPD/90283/2012).

References

[1] W. Blum and L. Rolandi, *Particle Detection with Drift Chambers*, Springer-Verlag, Berlin Germany (1994).

[2] G.F. Knoll, *Radiation detection and measurements*, John Wiley and Sons, Inc., New York U.S.A. (2000).

[3] F. Sauli, *Gaseous Radiation Detectors: Fundamentals and Applications*, Cambridge Monographs on Particle Physics, Nuclear Physics and Cosmology, Cambridge University Press, Cambridge U.K. (2014).

[4] G.A. Eiceman, Z. Karpas and H.H.J. Hill, *Ion Mobility Spectrometry*, third edition, CRC Press — Taylor & Francis Group (2014).

[5] A. Andronic, C. Garabatos, D. Gonzalez-Diaz, A. Kalweit and F. Uhlig, *A Comprehensive study of rate capability in Multi-Wire Proportional Chambers*, 2009 *JINST* **4** P10014 [arXiv:0909.0242].

[6] P.N.B. Neves, C.A.N. Conde and L.M.N. Távora, *Experimental measurement of the mobilities of atomic and dimer Ar, Kr, and Xe ions in their parent gases*, *J. Chem. Phys.* **133** (2010) 124316.

[7] Y. Kalkan, M. Arslandok, A.F.V. Cortez, Y. Kaya, İ. Tapan and R. Veenhof, *Cluster ions in gas-based detectors*, 2015 *JINST* **10** P07004.

[8] P.N.B. Neves, A.N.C. Garcia, A.M.F. Trindade, J.A.S. Barata, L.M.N. Távora and C.A.N. Conde, *Experimental measurement of the Ne^+ and Ne_2^+ mobilities in Ne and the reaction rate coefficient for $Ne^+ + 2Ne \rightarrow Ne_2^+ + Ne$*, *IEEE Trans. Nucl. Sci.* **58** (2011) 2060.

[9] A.N.C. Garcia, P.N.B. Neves, A.M.F. Trindade, F.P. Santos and C.A.N. Conde, *A new contribution to the experimental measurement of the N_4^+ ion mobility in N_2 at 298 K*, 2012 *JINST* **7** P02012.

[10] A.F.V. Cortez et al., *Experimental measurement of the mobility of ions originated in ethane in their parent gas*, 2013 *JINST* **8** P07013.

[11] A.F.V. Cortez et al., *Experimental measurements of the mobility of methane ions in Ar-C_2H_6*, 2013 *JINST* **8** P12012.

[12] A.N.C. Garcia, P.N.B. Neves, A.M.F. Trindade, A.F.V. Cortez, F.P. Santos and C.A.N. Conde, *Experimental ion mobility measurements in Xe-N_2 mixtures*, 2014 *JINST* **9** P07008.

[13] A.M.F. Trindade et al., *Experimental study on ion mobility in Ar-CH_4 mixtures*, 2014 *JINST* **9** P06003.

[14] P.M.C.C. Encarnação et al., *Experimental Ion Mobility measurements in Ar-CO_2 mixtures*, 2015 *JINST* **10** P01010.

[15] P.M.C.C. Encarnação et al., *Experimental Ion Mobility measurements in Ne-CO_2 and CO_2-N_2 mixtures*, 2016 *JINST* **11** P05005.

[16] A.F.V. Cortez et al., *Experimental ion mobility measurements in Ne-N_2*, 2016 *JINST* **11** P11019.

[17] A.F.V. Cortez et al., *Experimental ion mobility measurements in Xe-CO_2*, 2017 *JINST* **12** P06012.

2018 JINST 13 P11016

[18] A.M.F. Trindade et al., *Experimental studies on ion mobility in xenon-trimethylamine mixtures*, 2017 *JINST* **12** P07007.

[19] J.M.C. Perdigoto et al., *Experimental ion mobility measurements in Xe-CH_4*, 2017 *JINST* **12** P09003.

[20] J.M.C. Perdigoto et al., *Experimental ion mobility measurements in Xe-C_2H_6*, 2017 *JINST* **12** P10011.

[21] A.F.V. Cortez et al., *Experimental ion mobility measurements in Xe-CF_4*, 2018 *JINST* **13** P04006.

[22] M.A.G. Santos et al., *Experimental ion mobility measurements for the LCTPC collaboration — Ar-CF_4 mixtures*, 2018 *JINST* **13** P04012.

[23] National Institute of Standards and Technology, Gaithersburg, Maryland, 20899-8320 U.S.A. and online at http://physics.nist.gov/cuu/Constants/Table/allascii.txt.

[24] P. Langevin, *Une formule fondamentale de théorie cinetique*, *Ann. Chim. Phys.* **5** (1905) 245.

[25] E.W. McDaniel, J.B.A. Mitchell and M.E. Rudd, *Atomic collisions-heavy particle projectiles*, Wiley (1993).

[26] E.A. Mason and E.W. McDaniel, *Transport Properties of Ions in Gases*, John Wiley and Sons, Inc., New York U.S.A. (1988).

[27] K.M. Gough, M.M. Yacowar, R.H. Cleve and J.R. Dwyer, *Analysis of molecular polarizabilities and polarizability derivatives in H_2, N_2, F_2, CO, and HF, with the theory of atoms in molecules*, *Can. J. Chem.* **74** (1996) 1139.

[28] A. Blanc, *Recherches sur les mobilités des ions dans les gaz*, *J. Phys. Theor. Appl.* **7** (1908) 825.

[29] E.W. McDaniel and E.A. Mason, *The Mobility and Diffusion of Ions in Gases*, John Wiley & Sons, New York U.S.A. (1973).

[30] L.G. Christophorou, J. Olthott and P. Vassiliou, *Gaseous dielectrics X*, Springer Science + Business Media, New York U.S.A. (2004).

[31] A.M.F. Trindade et al., *Experimental measurements of the mobility of methane ions in methane*, 2012 *JINST* **7** P06010.

[32] J. Escada et al., *A Monte Carlo study of backscattering effects in the photoelectron emission from CsI into CH_4 and Ar-CH_4 mixtures*, 2007 *JINST* **2** P08001.

[33] Y. Itikawa, *Cross sections for electron collisions with nitrogen molecules*, *J. Phys. Chem. Ref. Data* **35** (2006) 31.

[34] T. Tabata, T. Shirai, M. Sataka and H. Kubo, *Analytic cross sections for electron impact collisions with nitrogen molecules*, *At. Data Nucl. Data Tables* **92** (2006) 375.

[35] H. Kutz and H.-D. Meyer, *Rotational excitation of N_2 and Cl_2 molecules by electron impact in the energy range* 0.01–1000 *eV: Investigation of excitation mechanisms*, *Phys. Rev. A* **51** (1995) 3819.

[36] G.J. Schulz, *Vibrational excitation of N_2, CO, and H_2 by electron impact*, *Phys. Rev.* **135** (1964) A988.

[37] A. Huetz, F. Gresteau and J. Mazeau, *'Dissociative attachment' in N_2*, *J. Phys.* **B 13** (1980) 3275.

[38] K. Hiraoka and T. Mori, *Formation and stabilities of cluster ions Ar_n^+*, *J. Chem. Phys.* **90** (1989) 7143.

[39] V.G. Anicich, *Evaluated bimolecular ion-molecule gas phase kinetics of positive ions for use in modeling planetary atmospheres, cometary comae, and interstellar clouds*, *J. Phys. Chem. Ref. Data* **22** (1993) 1469.

[40] D. Smith and N.G. Adams, *Charge-transfer reaction $Ar^+ + N \rightleftarrows N_2^+ + Ar$ at thermal energies*, *Phys. Rev.* **A 33** (1981) 2327.

2018 JINST 13 P11016

[41] A.A. Viggiano, J.M.V. Doren, R.A. Morris and J.F. Paulson, *Evidence for an influence of rotational energy on the rate constants for the reaction of* $Ar^+(^2P_{3/2})$ *with* N_2, *J. Chem. Phys.* **93** (1990) 4761.

[42] W. Hack et al., *Gmelin Handbook of lnorganic and Organametallic Chemistry*, Springer-Verlag (1993) [ISBN: 978–3–662–06335–4].

[43] P.A.M. van Koppen et al., *Ion-molecule association reactions: A study of the temperature dependence of the reaction* $N_2^+ + N_2 + M \rightarrow N_4^+ + M = N_2$, *Ne, and He: Experiment and theory*, *J. Chem. Phys.* **81** (1984) 288.

2018 JINST 13 P11016